

Polyphenol rich sugarcane extract restricts select respiratory viruses depending on their mode of entry

Caolingzhi Tang^a, Matthew Flavel^b, Sarah L. Londrigan^{a,*}, Jason M. Mackenzie^{a,**,1} 

^a Department of Microbiology and Immunology, The University of Melbourne at the Peter Doherty Institute for Infection and Immunity, 792 Elizabeth Street, Melbourne, VIC, 3000, Australia

^b The Product Makers (Australia) Pty Ltd, Keysborough, VIC, 3173, Australia

ARTICLE INFO

Keywords:

Influenza virus
Antiviral
Polyphenol
Respiratory virus
Virus replication
Endocytosis

ABSTRACT

We previously showed that Polyphenol rich sugarcane extract (PRSE) displayed significant inhibitory effect against influenza A virus (IAV). In this study, we investigated the mechanism of action (MOA) of PRSE against respiratory viruses in human-derived cells. We showed that PRSE treatment does not promote an antiviral state via expression of interferon stimulated genes (ISGs). We subsequently investigated any potential perturbation on the viral entry process and observed that PRSE treatment did not affect caveolin-mediated endocytosis but led to a significant attenuation in clathrin-mediated endocytosis. We confirmed this inhibitory effect on IAV entry, as infection was unaffected by PRSE when IAV fusion was induced at the plasma membrane, instead of endosomal membranes. Based on these findings we observed significant inhibitory effect of PRSE against respiratory syncytial virus and human metapneumovirus, which utilise clathrin-mediated endocytosis, but not human parainfluenza virus type 3, which fuses at the plasma membrane. In conclusion, we show that PRSE has broad antiviral activity and potentially perturbs virus entry via clathrin-mediated endocytosis to inhibit viral replication *in vitro*.

1. Introduction

In recent years, the rapid emergence and transmission of viruses has brought a heavy burden to human society with the impact most observable during the COVID-19 pandemic, caused by the Severe Acute Respiratory Syndrome-Coronavirus-2 (SARS-CoV-2) (Kavanagh et al., 2024; Mohamadian et al., 2021; Naseer et al., 2022). In the meantime, other respiratory viruses such as influenza A viruses (IAV), respiratory syncytial virus (RSV), human metapneumovirus (HMPV) and human parainfluenza viruses (PIV) are still circulating in the community and causing respiratory infections with increasing morbidity and mortality, especially in immunocompromised individuals (Griffiths et al., 2017; Peteranderl et al., 2016; Schuster and Williams, 2014). Some of these infections can be avoided with preventatives, such as immunization (Elliott et al., 2023; Schmoele-Thoma et al., 2022), but therapeutics (such as antivirals) are still desperately needed to combat and reduce the severity of severe viral infections in the infected patient.

Currently, there are more than a hundred antiviral therapies

approved by The United States Food and Drug Administration (FDA) against viral pathogens that cause infectious diseases, including SARS-CoV-2, herpes simplex virus (HSV), human immunodeficiency virus (HIV), hepatitis B virus (HBV) and IAV (Tompa et al., 2021). These antivirals either modulate cellular responses (e.g. Pegylated interferon- α (IFN) for hepatitis B virus chronic infection) or impede the virus replication process (e.g. Baloxavir for IAV treatment) to achieve an effective inhibitory effect against the target viruses (Kumari et al., 2023; Ye and Chen, 2021). However, despite the advancement in antiviral research, there is still a huge gap in effective treatment to reduce the disease severity associated with many other respiratory viruses such as HMPV and human parainfluenza virus type 3 (PIV-3). Moreover, most antivirals are directed towards pathogen-specific targets, which contributes to the ongoing emergence of antiviral resistance for specific viruses. For example, the H275Y mutation in IAV that emerged in 2007 is associated with a conformational change to the active site of neuraminidase (NA) and led to resistance to NA inhibitor oseltamivir (Lampejo, 2020). Additionally, a thymidine kinase (TK) gene mutation in HSV affects the

* Corresponding author.

** Corresponding author.

E-mail addresses: sarahll@unimelb.edu.au (S.L. Londrigan), jason.mackenzie@unimelb.edu.au (J.M. Mackenzie).

¹ Both authors contributed equally to this work.

enzymatic activity of TK and promoted resistance to acyclovir (Schalkwijk et al., 2022). Therefore, there's an urgent need to identify and develop novel antivirals that potentially target cellular responses and/or pathways to reduce the opportunity for resistance.

Polyphenol rich sugarcane extract (PRSE) is an extract prepared from sugarcane molasses by The Product Makers using a patented hydrophobic extraction method (Deseo et al., 2020). PRSE was previously reported with anti-inflammatory properties by the inhibition of tumor necrosis factor α (TNF- α) and the activation of nuclear factor erythroid 2-related factor 2 (Nrf2) pathways and physiological benefits (Ahtesh et al., 2020; Ji et al., 2019, 2020; Prakash et al., 2021). A liquid chromatography – mass spectrometry (LC-MS) analysis previously revealed that PRSE had a complex composition with more than 13 polyphenols detected, including chlorogenic acid, triclin, luteolin and apigenin (Ji et al., 2019). These polyphenols have been previously associated with antiviral activities against different viruses such as IAV (Ding et al., 2017), human cytomegalovirus (CMV) (Itoh et al., 2018; Murayama et al., 2012) and RSV (Wang et al., 2020). The complex polyphenol composition of PRSE therefore provides potential to act as a broad-spectrum antiviral agent.

Our previous study identified an antiviral activity for PRSE *in vitro* against multiple IAV strains in Madin-Darby canine kidney (MDCK) cells (Tang et al., 2024). In addition, we identified that the antiviral activity of PRSE was effective during the early stages of IAV replication. We observed that treatment with PRSE did not alter the morphology of IAV directly nor the ability of the virus to attach to sialic acid on the surface of cells. Herein, we aimed to further interrogate the antiviral properties of PRSE against IAV, including investigation into the potential mechanism of action (MOA) against IAV. We sought to determine if PRSE treatment impacted either the host cellular antiviral response or specific stages of the viral replication cycle. We additionally determined if PRSE was equally effective against other respiratory viruses associated with significant disease burden in humans.

2. Materials and methods

2.1. Cells

The A549 human lung epithelial cell line (obtained from the American type culture collection (ATCC)), Manassas, VA, USA) was maintained and passaged in Kaighn's modification of Ham's F-12K medium (Gibco, Thermo Fisher Scientific, Waltham, MA, USA) supplemented with 10 % (v/v) heat-inactivated foetal bovine serum (FBS) (GE Healthcare Life Sciences, Utah, USA), 2 mM L-glutamine (Gibco), 1 % (v/v) sodium pyruvate (Gibco), 100 units/mL penicillin, and 100 μ g/mL streptomycin (Gibco) at 37°C in 5 % CO₂. Madin-Darby canine kidney (MDCK) cells (ATCC) were maintained and passaged in RPMI 1640 Medium (Gibco) supplemented as above at 37°C, 5 % CO₂. Human epithelial type 2 (Hep-2) cells were maintained and passaged in Dulbecco's Modified Eagle Medium (DMEM; Gibco) containing 1 g/L glucose and supplements as above, at 37°C in 5 % CO₂.

2.2. Viruses

The influenza A virus X-31 (H3N2) with the PB1, PB2, NP, PA, M and NS gene segments of A/Puerto Rico/8/34 (PR8) and the HA and NA gene segments of A/Aichi/2/68 used in this study was provided as allantoic fluid by Prof Patrick Reading from the World Health Organisation Collaborating Centre for Reference and Research on Influenza (WHO CCRR) at the Doherty Institute, Melbourne. RSV Long (VR-26) was purchased from the ATCC. Virus stock was generated by propagation in Hep-2 cells. Briefly, Hep-2 cells were infected with RSV Long until syncytium formation was observed in 50 % of the cells. Both cells and supernatant were harvested and freeze-thawed to release intracellular viruses before the centrifugation to remove the cell debris (Chan et al., 2018). The generated virus stock was then titrated by virospot assay

described as below. The CAN97-83 HMPV strain was a kind gift from Professor Kirsten Spann (Queensland University of Technology, Australia) and was propagated in LLC-MK2 cells at 32°C in the presence of 5 μ g/ml tosylsulfonyl phenylalanyl chloromethyl ketone (TPCK) trypsin (Worthington Biochemical, NJ, USA), as previously described (Gillespie et al., 2016). PIV-3 strain C243 was obtained from the ATCC (VR1540) and propagated in LLC-MK2 cells as previously described (Meischel et al., 2021).

2.3. PRSE

PRSE was extracted from sugarcane molasses using a patented hydrophobic extraction process by The Product Makers Pty Ltd (Ji et al., 2019, 2020) and stored at room temperature (RT). The PRSE compound was reconstituted at 10 mg/ml in serum-free medium (Kaighn's modification of Ham's F-12K) and filtered through a 0.22 μ m syringe. Filtered PRSE was aliquoted and stored at -20°C. The cytotoxicity of PRSE in A549 cells was measured by flow cytometric analysis. A549 cells were incubated at 37°C, 5 % CO₂, with various concentrations of PRSE for 24h before detached by trypsinization and staining with eBioscience™ Fixable Viability Dye eFluor™ 780 (Invitrogen, Waltham, Massachusetts, USA). Samples were then fixed with 4 % (v/v) paraformaldehyde (PFA) in PBS and analysed on a FACSCanto II (BD Biosciences, CA, USA) before data analysis using FlowJo software (version 10.4).

2.4. Virus infection

Virus inoculum (IAV/RSV/HMPV/PIV-3) was pre-treated with 1 mg/mL PRSE or serum-free media (for mock-treated virus) for 1h at 37°C before infection of A549 cells. A549 cell monolayers were cultured in 24-well tissue culture plates (Corning, New York, USA) overnight to 70 % confluency before infection with virus. Cells were exposed to pre-treated virus in the presence of 1 mg/mL PRSE or serum-free media (mock) for 1h at 37°C in 5 % CO₂. The inoculum was then removed, and cells were washed with phosphate buffered saline (PBS) to remove residual input virus before maintenance in media containing 1 mg/mL PRSE or serum-free media (mock) at 37°C, 5 % CO₂. Media was also supplemented with 0.5 μ g/mL TPCK-treated trypsin when IAV multi-cycle replication was being assessed. IAV-infected cells were harvested at 8 h post infection (hpi) for flow cytometry analysis. Cell-free supernatants (IAV infection) were harvested at 24hpi for further titration by plaque assay. RSV, HMPV and PIV-3 infected cells were harvested at 30hpi by gentle scraping, where cells and supernatants were snap-frozen, thawed and centrifuged to remove cell debris before titration by virospot assay.

2.5. Plaque assay

MDCK cell monolayers were cultured in 6-well tissue culture plates (Corning, New York, USA) overnight to reach 100 % confluency. Media was replaced with serum-free media before infecting with diluted virus inoculum. After 45 min incubation at 37°C, 5 % CO₂, 3 mL of overlay containing Leibovitz's L-15 Medium (Gibco), 0.9 % (w/v) agarose (Sigma-Aldrich, St. Louis, Missouri, USA) and 0.5 μ g/mL TPCK treated trypsin was added to the infected cells and incubated for 72h at 37°C, 5 % CO₂ before identification of plaques.

2.6. Virospot assay

Briefly, Hep-2 cell monolayers were cultured in 96-well tissue culture plates (Corning, New York, USA) overnight to reach 100 % confluency. Cells were washed with PBS before infection with 100 μ L virus inoculum for 1h at 37°C in 5 % CO₂. Infected cells were overlaid with 100 μ L of 3.2 % (w/v) carboxymethyl cellulose (CMC) (Sigma-Aldrich) in DMEM. Infected cells were incubated for 48h before fixation with 80 % (v/v) acetone for 10 min at 4°C. 0.5 μ g/mL TPCK-treated trypsin was

added to the HMPV overlay to facilitate multi-cycle replication. RSV virospots were detected as described previously (Chan et al., 2018) using an RSV-specific human antibody kindly provided by Dr Keith Chappell (University of Queensland) in conjunction with goat anti-human IgG (H + L) HRP conjugate. HMPV virospots were identified using a mouse antibody that is specific for HMPV F protein (Merck, Australia). PIV-3 virospots were detected by a mouse anti-PIV-3 HN antibody (Abcam) in conjunction with rabbit anti-mouse IgG conjugated with HRP as described (Meischel et al., 2021). Subsequently, TrueBlue peroxidase substrate (SeraCare) was added to allow for colour development before being dried and read and counted by CTL-Immunospot S6 Macro analyzer with CTL Switchboard 2.6.0 (x86).

2.7. Detection of IAV nucleoprotein expression by flow cytometry

PRSE-treated and IAV-infected A549 cells as well as mock-treated IAV-infected A549 cells were detached by trypsinization and stained with eBioscience™ Fixable Viability Dye eFluor™ 780 (Invitrogen) before fixation with 4 % (v/v) paraformaldehyde (PFA) in PBS. After fixation, cells were permeabilised with 0.5 % (v/v) Triton-X-100 in PBS and stained with mouse anti-IAV NP antibody conjugated with FITC (MA1-7322, Invitrogen). Samples were analysed on a FACSCanto II (BD Biosciences, CA, USA) before data analysis using FlowJo software (version 10.4). Geometrical mean fluorescence intensity (gMFI) of IAV NP was quantitated on IAV NP-positive cell population.

2.8. Detection of STAT1 protein by western blot

A549 cells were incubated with 1 mg/mL PRSE diluted in serum-free media or serum-free media (mock) for 24h before addition of 853 U/mL IFN- α 2A (Sapphire Bioscience, NSW, Australia) in media containing 1 mg/mL PRSE (or serum-free media (mock)). A549 whole cell lysates were harvested after 1h incubation at 37°C, 5 % CO₂, using 1 % (v/v) NP40 cell lysis buffer (Invitrogen) with 10 % (w/v) PhosSTOP™ (Roche, Basel, Switzerland) and 0.1 % (v/v) protease inhibitor Cocktail III (Astral Scientific, NSW, Australia). Samples were reduced with 5 % (v/v) 2-Mercaptoethanol (Gibco) and heated to 90°C for 5 min before separation by SDS-PAGE using precast 4–15 % gradient gels (Thermo Fisher Scientific, MA, USA), followed by transfer to polyvinylidene difluoride (PVDF) membrane (Thermo Fisher Scientific). Membranes were blocked in PBS with 5 % (w/v) bovine serum albumin (Sigma-Aldrich) and 0.05 % (v/v) Tween 20 (Sigma-Aldrich). All subsequent washes and antibody binding steps were performed in TBS containing 0.1 % (v/v) Tween 20. The cellular protein β -actin (approximately 48 kDa in size) was visualised as a loading control using mouse monoclonal antibody specific for β -actin (santsc-47778, VWR, Pennsylvania, USA) in conjunction with rabbit anti-mouse IgG-horseradish peroxidase (HRP) (AB6728, Abcam, Cambridge, UK). STAT1 protein, phosphorylated STAT1 protein and IAV M1 protein were detected using rabbit anti-STAT1 antibody (AHO0832, Invitrogen), mouse anti-phosphorylated STAT1 antibody (#612132, Becton Dickinson, VIC, Australia) or mouse anti-IAV M1 antibody (MA401, BioRad, USA) in conjunction with rabbit anti-mouse IgG-HRP (AB6728, Abcam) or goat anti-rabbit IgG-HRP (AB6721, Abcam) and visualised by enhanced chemiluminescence (ECL) using Western Lightning Ultra (PerkinElmer, VIC, Australia) with an Amersham ImageQuant 800 Western Blot Imaging System (GE Healthcare Life Sciences, Utah, USA).

2.9. Detection of interferon-stimulated genes (ISGs) by qRT-PCR

A549 cells were incubated with 1 mg/mL PRSE diluted in serum-free media and serum-free media (mock) for 24h before addition of 853 U/mL IFN- α 2A in media containing 1 mg/mL PRSE (or serum-free media (mock)). Whole cell lysates were harvested for RNA extraction 6h or 24h after IFN- α 2A addition by lysis with Trizol. cDNA was prepared using the Tetro cDNA synthesis kit according to manufacturer's instructions

(Bioline, TN, USA) in conjunction with Oligo DT primer for synthesis of mRNA. qRT-PCR was performed using the SensiFAST 2x SYBR Lo- Rox kit (Bioline) with primer pairs specific for human MxA gene (Fwd: GGCTGTTTACCAGACTCCGACA; Rev: CACAAAGCCTGG-CAGCTCTCTA), OAS gene (Fwd: CTGATGCAGGAACGTATAGCAC; Rev: CACAGCGTCTAGCACCTTT) and IFITM3 gene (Fwd: ATCGT-CATCCCAGTGCTGAT; Rev: ACGTGGGATACAGGTCATGG). Human GAPDH expression (Fwd: TGAAGGTCGGAGTCAACGG; Rev: GGCAA-CAATATCCACTTTACCAGAG) was used for normalisation. Data acquisition and analysis was performed using the QuantStudio 7 Flex Real-Time PCR System and Design and analysis software (Applied Biosystems, Waltham, MA, USA).

2.10. Cholera toxin B (CTB)/transferrin entry assay

A549 cells were seeded on coverslips (Bio-strategy, Tullamarine, Australia) and incubated overnight to reach 60 % confluency. Cells were pre-treated with media containing 1 mg/mL PRSE or serum-free media (mock) for 2h or 50 μ M dynasore (Abcam), 10 μ g/mL chlorpromazine (CPZ) (Sigma-Aldrich) or 80 μ g/mL genistein (Thermo Fisher Scientific) for 30min at 37°C, then washed with ice-cold PBS. Cholera toxin B (CTB) conjugated to Alexa Fluor™ 647 (CTB-AF647; C34778, Thermo Fisher Scientific) at 3 μ g/mL or transferrin conjugated to Alexa Fluor™ 647 (TF-AF647; 009-600-050, Life technologies, Carlsbad, California, USA) at 40 μ g/mL in serum-free media containing 1 mg/mL PRSE, 50 μ M dynasore, 10 μ g/mL CPZ, 80 μ g/mL genistein or serum-free media (ice-cold) were added and incubated at 4°C for 10 min. Cell monolayers were washed with ice-cold PBS to remove unbound ligand before addition of pre-warmed (37°C) serum-free media containing 1 mg/mL PRSE, 50 μ M dynasore, 10 μ g/mL CPZ, 80 μ g/mL genistein or serum-free media (mock) and incubated for 15–30 min (TF-AF647) or 45 min (CTB-AF647) at 37°C in 5 % CO₂ for ligand entry. Controls cells held at 4°C were washed with ice-cold PBS and incubated with ice-cold media containing 1 mg/mL PRSE, 50 μ M dynasore, 10 μ g/mL CPZ, 80 μ g/mL genistein or serum-free media for 30 min (TF-AF647) or 45 min (CTB-AF647) at 4°C to retain ligands on cell surface. Cells were fixed with 4 % (v/v) PFA before subsequent staining with Hoechst33342 (H1399, Life technologies, Carlsbad, California, USA). A549 cells from the CTB-AF647 entry assay were also stained with rabbit polyclonal antibodies to Giantin (ab80864, Abcam) for detection of the Golgi Apparatus in conjunction with donkey-anti rabbit-Alexa Flour 488 (A21206, Life technologies). Confocal immunofluorescence microscopy was used to visualise ligands bound to the cell surface or internalised.

2.11. IAV infection induced by fusion at the plasma membrane

In experiments to facilitate IAV infection via fusion with the plasma membrane, A549 cell monolayers were washed and incubated in serum-medium containing 10 mM NH₄Cl (Chem-supply, SA, Australia) for 30 min at 4°C before exposure to IAV pre-treated with PRSE (MOI 1) for 1h at 4°C to enable binding to the cell surface. Cells were then washed extensively with ice-cold PBS and incubated in serum-free media (mock) or fusion buffer (20 mM HEPES, 2 mM CaCl₂, 150 mM NaCl, 20 mM citric acid monohydrate-sodium citrate tribasic dehydrate, pH 5.0) for 10 min at 37°C to promote virus fusion with the plasma membrane. The fusion buffer was then removed and replaced with serum-free medium containing 10 mM NH₄Cl with or without 1 mg/mL PRSE. A549 cells were then maintained at 37°C in 5 % CO₂ for 8h. Cells were then analysed for IAV infection by flow cytometry or immunofluorescence microscopy.

2.12. Confocal immunofluorescence microscopy

A549 cell monolayers grown on coverslips were fixed with 4 % (v/v) PFA and blocked with 0.1 M glycine and 5 % (w/v) bovine serum albumin (BSA) with 5 % FBS (v/v) in PBS. Cells were then permeabilised

with 5 % (v/v) Triton-X-100 in PBS and nucleus were stained with Hoechst33342. IAV-infected cells were stained with mouse monoclonal anti-NP-FTIC antibody (Invitrogen). Coverslips were mounted on glass-slides with Prolong Diamond antifade mountant (P369665, Thermo Fisher Scientific) and left to dry overnight at RT. Slides were then stored at 4°C and cells were analysed using a Zeiss 780 Confocal Microscope and Zen™ Zeiss® software and an Image J software. Pearson correlation coefficients were measured between CTB-AF647 and Giantin staining, indicating the degree of co-localization. Average TF-AF647 intensity per cell in each field was quantitated to indicate the uptake of transferrin.

2.13. Statistical analysis

Graph presentation and statistical analysis of data was performed using GraphPad Prism (GraphPad Software, San Diego, CA). Statistical significance was calculated using an unpaired, two-tailed *t*-test or non-parametric Mann-Whitney test as indicated.

3. Results

3.1. PRSE inhibits IAV replication in A549 cells

Previously we reported that PRSE was antiviral against IAV in MDCK cells (Tang et al., 2024), however, the effect of PRSE in human cell lines was not determined. In this study, we aimed to evaluate the antiviral activity of PRSE in the human A549 lung epithelial cell line. Based on our previous study (Tang et al., 2024), we confirmed that treatment of A549 cells with 1 mg/mL PRSE displayed no cytotoxic effect (Fig. S1). To assess the antiviral activity of PRSE in IAV-infected A549 cells, we pre-treated the IAV inoculum with PRSE for 1h before infection and PRSE was maintained in the media throughout the course of the infection. The PRSE-treated A549 cells were infected with IAV at various multiplicities of infection (MOI) (0.1, 0.5 and 1), and cell-free supernatants were harvested at 24hpi before released infectious virus was measured by plaque assay (Fig. 1A and B). We observed that PRSE treatment inhibited IAV infectious virus production in A549 cells at all the tested MOI (Fig. 1A). The greatest inhibitory effect of $91.3\% \pm 1.7\%$ inhibition was observed when cells were infected with an MOI of 0.1 (Fig. 1B), whereas infections at an MOI of 0.5 and 1.0 resulted in reductions of $83.8\% \pm 2.1\%$ and $81.1\% \pm 5.0\%$, respectively (Fig. 1B).

To further confirm and characterise the antiviral activity of PRSE in IAV-infected A549 cells, flow cytometric analysis was performed to evaluate IAV infection levels by measuring the expression of newly synthesised IAV nucleoprotein (NP) (Fig. 1C and D). From our analyses, we observed a significant reduction in the percentage of IAV NP-positive cells (Fig. 1C and D) and a significant reduction in the geometrical mean fluorescent intensity (gMFI) of IAV NP expression in IAV NP-positive cells (indicative of NP protein expression levels in infected cells) after PRSE treatment at 8hpi for all tested MOI (Fig. 1E). Here the most significant reduction could be observed at an MOI of 1, where a $>50\%$ reduction in the percentage of NP positive cells and $\sim 20\%$ reduction in the gMFI of IAV NP expression in IAV NP-positive cells were observed (Fig. 1D).

Overall, the above findings indicate that PRSE has inhibitory activity against IAV replication in the human A549 cell line. It also confirms our previous observations indicating that PRSE treatment reduced IAV infectious virus production due to limiting the early stages of the viral replication cycle, as determined by a reduction in the number of cells expressing IAV viral NP coupled with attenuated IAV NP protein expression in IAV-infected cells.

3.2. PRSE enhanced the IFN-stimulated phosphorylation of STAT1 protein but did not modulate the expression of select interferon-stimulated genes (ISGs)

Given the observed inhibitory effect of PRSE against IAV replication

in A549 cells, we aimed to further investigate the underlying mechanism of action (MOA). We initially investigated if PRSE treatment acted on host cells to induce cellular antiviral responses to impart an antiviral state against IAV. The Janus kinase/signal transducer and activator of transcription (JAK/STAT) signalling pathway is one of the most important immune communication pathways and plays an important role in initiating cellular antiviral response through the induction of interferons (IFN) and interferon stimulated genes (ISGs) (Hu et al., 2021). Thus, we incubated A549 cells in media with or without 1 mg/mL PRSE for 24h before stimulation with type I IFN for 1h for evaluation of STAT1 expression and phosphorylation at the protein level, and at 6 or 24h for assessment of mRNA expression for select ISGs. We chose MxA, OASL and IFITM3 as they are known for their antiviral properties against IAV (Husain, 2024; Xiao et al., 2013).

We observed that PRSE- and mock-treated cells were unaltered in the level of total STAT1 protein expression, regardless of the treatment by type I IFN (Fig. 2A). Additionally, in the absence of type I IFN stimulation, neither the PRSE- or mock-treated cells had detectable phosphorylated STAT1 protein expression (Fig. 2A). This observation indicated that PRSE treatment alone does not induce the phosphorylation of STAT1 protein contributing to the antiviral effect. Conversely, we did observe a mild increase in phosphorylated STAT1 protein in the PRSE-treated cells additionally stimulated with type I IFN (Fig. 2A–C). Compared to the mock-treated cells, PRSE-treated cells had an approximate 50 % increase in phosphorylated STAT1 protein expression (Fig. 2C). Moreover, a similar effect was observed in the context of IAV infection, where STAT1 levels remained similar but phosphorylation of STAT1 was enhanced by PRSE treatment upon IFN- α 2A stimulation (Supplementary Fig. 2). This suggests that PRSE treatment may enhance the signalling capacity of type I IFN, promoting increased phosphorylation of the STAT1 protein in A549 cells.

As we had observed that PRSE treatment resulted in an increase in phosphorylated STAT1 protein we aimed to determine if this contributed to an increase in ISG expression. Thus, A549 cells were treated (or not) with PRSE and the relative expression of mRNA for MxA, OASL and IFITM3 compared to GAPDH (house-keeping gene) was evaluated at 6 and 24h post type I IFN treatment (Fig. 2D and E). We observed that the PRSE-treated cells had similar expression levels of MxA, OASL and IFITM3 mRNA to that of mock-treated cells at all time points in the absence of type I IFN (Fig. 2C and D). Treatment with type I IFN for either 6 or 24h resulted in a significant increase in MxA, OASL and IFITM3 mRNA expression in both PRSE-treated and mock-treated A549 cells indicating STAT1 signalling leading to ISG induction (Fig. 2C). Notably, there was no significant difference in MxA, OASL or IFITM3 mRNA expression level in the presence or absence of PRSE- and/or type I IFN at either time point (Fig. 2C and D).

Our combined observations suggest PRSE treatment alone does not stimulate phosphorylation of STAT1, nor does it promote the induction of expression of select ISG mRNA. However, we did observe that PRSE treatment increased the amount of phosphorylated STAT1 in the presence of type I IFN, but this did not appear to directly enhance the ISG response.

3.3. PRSE treatment does not affect the caveolin-mediated uptake of cholera toxin B (CTB)

After observing that no major antiviral state was established in A549 cells by exposure to PRSE treatment, we aimed to investigate how the IAV replication cycle was impacted by PRSE. From our previous study, we observed that PRSE most likely acts on an early stage of the IAV replication cycle following virus attachment. Thus, we initially aimed to determine whether virus entry was impacted by PRSE treatment.

There are three main pathways that enveloped viruses utilise to enter host cells, which are fusion at the cell surface, caveolin-mediated endocytosis and clathrin-mediated endocytosis. To investigate the potential PRSE-mediated perturbation of caveolin-mediated endocytosis

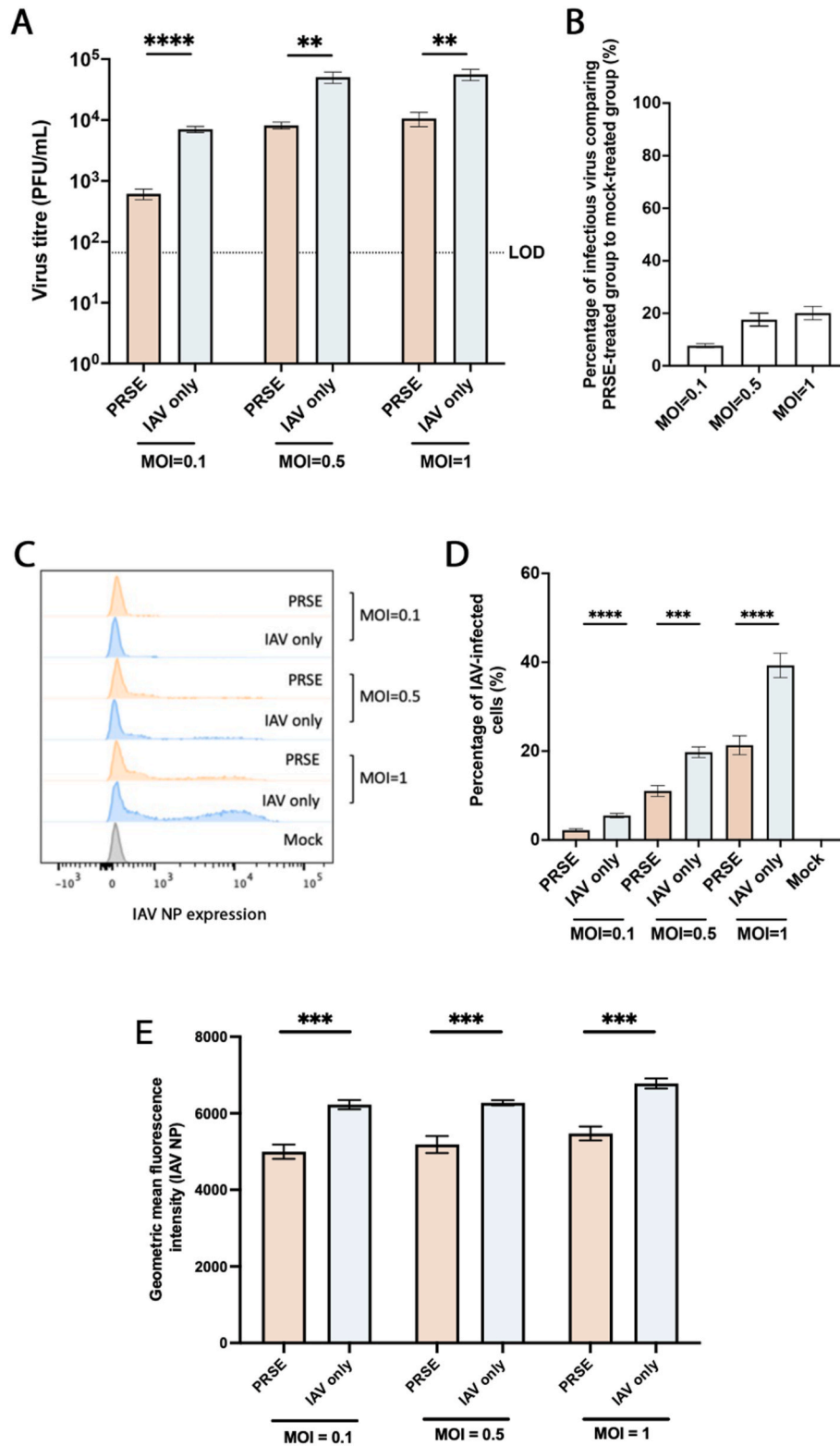


Fig. 1. PRSE has antiviral activity against influenza A virus replication in human-derived cells *in vitro*. A549 cells pre-treated with 1 mg/mL PRSE were infected with IAV X31 (H3N2) at various MOIs (0.1, 0.5 and 1) and then maintained in culture media with 1 mg/mL PRSE for the duration of the infection. **(A)** Infectious viruses present in cell-free supernatants harvested at 24hpi was titrated by plaque assay and expressed as plaque forming units/ml (PFU/mL). N = 3 independent experiments performed in triplicate. **(B)** The antiviral effect of PRSE at different MOI was assessed by comparing IAV infectious virus production in PRSE-treated and mock-treated cells. **(C)–(E)** The antiviral effect of PRSE was assessed by comparing **(D)** the percentage of IAV NP-positive cells and **(E)** the GMFI of IAV NP expression in the IAV NP-positive cell population at 8hpi in PRSE-treated and mock-treated A549 cells by flow cytometric analysis. N = 3 independent experiments performed in triplicate. **(A, B, D and E)** Error bars = SEM, ***p < 0.001, ****p < 0.0001 by unpaired two-tailed *t*-test.

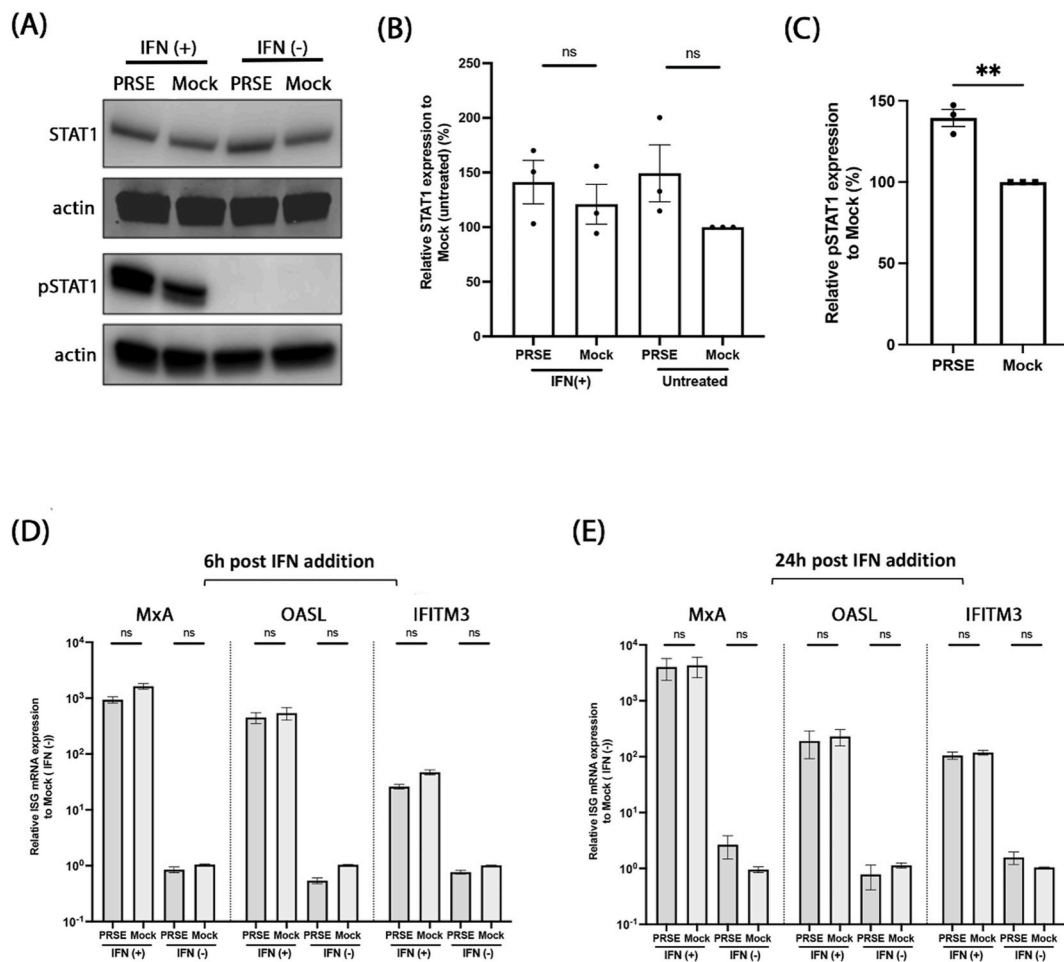


Fig. 2. PRSE treatment does not impact on ISG signalling alone but enhances the phosphorylation of STAT1 protein in the presence of IFN- α . (A) Western blot of whole A549 cell lysates with or without PRSE treatment for 24h with or without IFN- α 2A stimulation for an additional 1h. Membranes were probed with antibodies to STAT1 (84 kDa), phosphorylated STAT1 (pSTAT1) (84 kDa and 91 kDa) and β -Actin (48 kDa, as a protein loading control). Bound antibodies were detected with HRP-conjugated secondary antibodies and visualised by ECL. A representative Western blot from three independent experiments is shown. (B) Quantitation of STAT1 protein is expressed as relative STAT1 expression compared to mock-treated and IFN-unstimulated cells after normalisation against β -Actin expression. (C) Quantitation of phosphorylated STAT1 protein is expressed as relative phosphorylated STAT1 expression to mock-treated and IFN-stimulated cells after normalisation against β -Actin expression. (D) and (E) MxA, OASL and IFITM3 mRNA levels were quantitated by qRT-PCR at 6 and 24h post IFN- α 2A treatment of A549 cells. For MxA, OASL and IFITM3, $n = 3$ independent experiments performed in triplicate, error bars = SEM, ns = not significant by non-parametric Mann-Whitney test or $**p < 0.01$, by unpaired two-tailed t -test.

we used a surrogate assay whereby A549 cells were incubated with fluorescently labelled cholera toxin B (CTB-AF647) whereby endocytosis and trafficking to the Golgi apparatus can be tracked by confocal immunofluorescence microscopy (Wernick et al., 2010). Thus, PRSE-treated or untreated A549 cells were incubated on ice for 10 min with or without CTB-AF647. The cells were subsequently warmed to 37°C for 45 min and transport of the CTB-AF647 to the Golgi apparatus was determined by co-localization with antibodies specific to a resident protein of the Golgi apparatus, Giantin (Fig. 3). We observed that CTB-AF647 was retained at the surface of plasma membrane at 4°C in both the PRSE- and mock-treated cells (Fig. 3A ii, v, viii, xi and Fig. 3B ii, v, viii, xi). In addition, no signal for CTB-AF647 was detected in groups without the ligand (Fig. 3Aiii, xii and 3Biii, xii). Following 45 min incubation at 37°C, the CTB-AF647 was observed to enter and co-localise with anti-Giantin antibodies in the Golgi apparatus in mock-treated cells (Fig. 3A i, iv, vii, x and 3C). A very similar finding was made in the PRSE-treated cells where clear transport of CTB-AF647 to the Golgi apparatus is also observed (Fig. 3A i, iv, vii, x and 3C). No statistical difference was observed in the co-localization coefficient of CTB-AF647 and Giantin between PRSE treated cells and mock treated cells (Fig. 3C).

These observations would indicate that the uptake of CTB-AF647

was not affected by PRSE treatment, suggesting that PRSE treatment poses no impediment on the process of caveolin-dependant endocytosis in A549 cells.

3.4. PRSE treatment perturbs the uptake of transferrin via clathrin-mediated endocytosis

As we had shown that caveolae-dependent endocytosis was not perturbed by PRSE treatment, we aimed to investigate another viral entry pathway, namely clathrin-mediated endocytosis. Like CTB-AF647, AF647-conjugated transferrin (TF-AF647) was used as a surrogate to evaluate clathrin-mediated endocytosis. We incubated cells with TF-AF647 on ice for 10 min, before warming to 37°C for 15 or 30 min. Internalised TF-AF647 was then observed by confocal microscopy and quantitated (Fig. 4). As expected, at 4°C, the TF-AF647 remained at the cell surface in both the PRSE- and mock-treated cells (Fig. 4A iii, vii, xi and Fig. 4B ii, vii, xi). In mock-treated cells we observed bright aggregates of the TF-AF647 within the cell cytoplasm after 15 or 30 min incubation at 37°C (Fig. 4B i, ii, v, vi, ix, x). In contrast, we observed that in the PRSE-treated cells a weaker or almost no existent TF-AF647 signal could be observed in the cytoplasm (Fig. 4A i, ii, v, vi, ix, x).

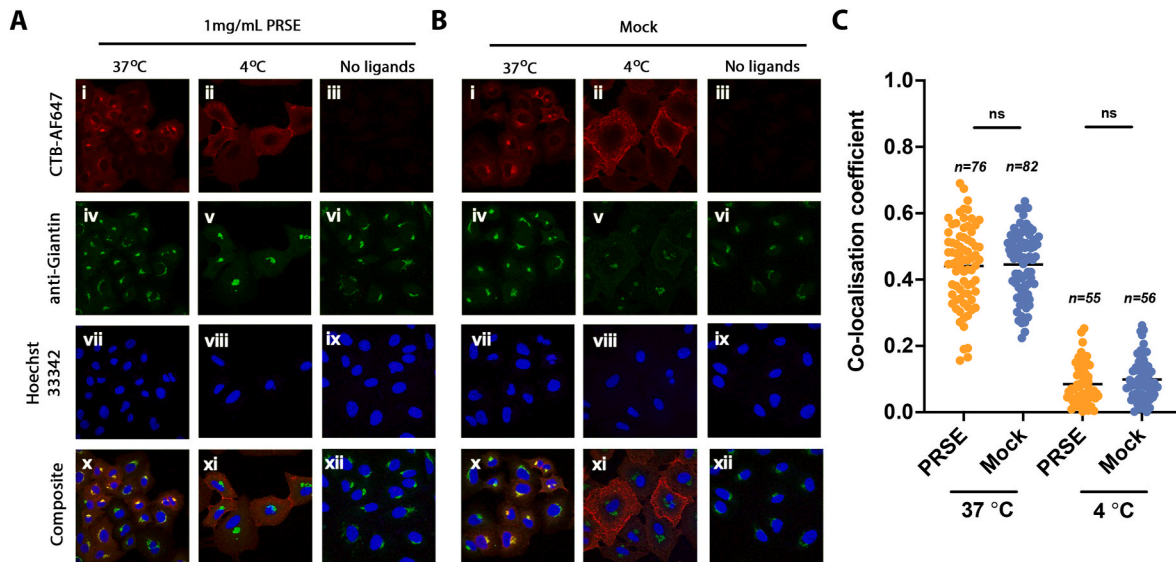


Fig. 3. PRSE treatment does not affect the uptake of cholera toxin B (CTB) via caveolae-mediated endocytosis. (A) and (B) A549 cells were treated or not with 1 mg/mL PRSE, fixed with PFA after different incubation conditions (4°C and 37°C) and the entry of CTB conjugated to AlexaFluor-647 (CTB-AF647) was visualised following co-staining with anti-Giantin antibodies visualised with anti-rabbit AlexaFluor-488. Hoechst 33342 staining was used to visualise nuclei before examination by confocal microscopy at 63x magnification. (C) Pearson correlation coefficients were determined for CTB-AF647 signal and Giantin staining, indicating the degree of co-localization. N = 55–82 cells from multiple fields from two independent experiments. Ns = not significant, by unpaired two-tailed *t*-test.

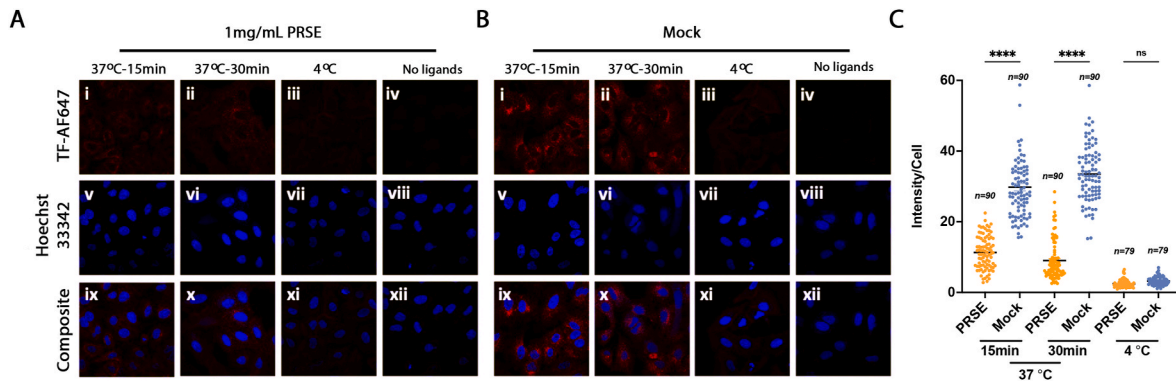


Fig. 4. PRSE treatment perturbs the internalisation of transferrin via clathrin-mediated endocytosis. (A) and (B) A549 cells were incubated in the presence or absence of 1 mg/mL of PRSE and fixed with 4 % PFA 15 min or 30 min after the entry of transferrin conjugated to AlexaFluor-647 (TF-AF647) before co-staining with Hoechst 33342 and examination by confocal microscopy at 63x magnification. (C) Average transferrin intensity per cell in each field was quantitated using Image J software. N = 79–90 cells from multiple fields from three independent experiments. *****p* < 0.0001, by unpaired two-tailed *t*-test.

Quantitation of transferrin intensity per cell in images clearly indicates a significant impairment in the uptake of TF-AF647 in PRSE-treated cells after both 15 and 30 min at 37°C (Fig. 4C). In addition, we also utilized an additional panel of endocytosis inhibitors, including dynasore (both clathrin-mediated endocytosis inhibitor and caveolin-mediated endocytosis inhibitor), CPZ (clathrin-mediated endocytosis inhibitor) and genistein (caveolin-mediated endocytosis inhibitor) to assess the specificity of transferrin uptake, which serves as a representative marker for clathrin-mediated endocytosis. We observed attenuated uptake of transferrin following the treatment of PRSE, dynasore and CPZ at 37°C while no blockage of transferrin uptake was observed in genistein-treated cells and mock-treated cells (Supplementary Fig. 3).

Overall, these data indicate that PRSE treatment appears to perturb and delay the uptake of transferrin into cells. As IAV utilises clathrin-mediated endocytosis as the major pathway to enter host cells (Mazel-Sanchez et al., 2023), this result would suggest that the observed antiviral activity of PRSE towards IAV may be related to a potential impediment on the process of virus entry.

3.5. The inhibitory effect of PRSE against IAV is attenuated in an entry-bypass infection where fusion occurs at the plasma membrane

As we had observed that the impact of PRSE treatment may influence clathrin-mediated endocytosis (Fig. 4), we aimed to utilise a plasma membrane acid bypass assay which promotes IAV fusion at the plasma membrane rather, than entry via clathrin-mediated endocytosis. Our hypothesis was that PRSE should not be antiviral against IAV when viral entry occurs at the plasma membrane. To perform this experiment, A549 cells were pre-treated with 10 mM NH₄Cl to prevent the acidification of endosomes and block virus entry via endocytosis. Cells were then exposed to IAV at 4°C to facilitate virus binding, before incubation with fusion buffer (pH = 5.0) at 37°C, to promote virus fusion with the plasma membrane and subsequent virus entry.

As expected, PRSE treatment itself reduced the percentage of IAV-infected cells by 25 % at 8hpi when infection occurred via the normal endocytic pathway (Fig. 5A–C). Treatment of A549 cells with NH₄Cl to prevent the acidification of endosomes, resulted in an almost complete inhibition of IAV infection consistent with entry via clathrin-mediated

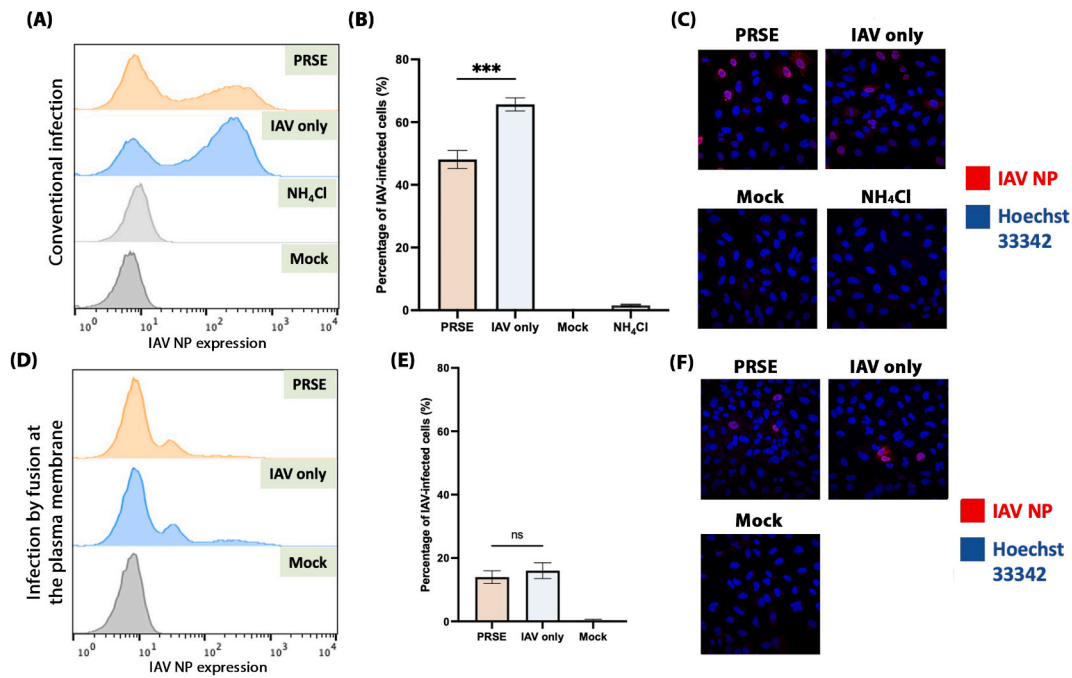


Fig. 5. The inhibitory effect of PRSE against IAV is attenuated in an entry-bypass infection. A549 cells were infected with IAV at MOI of 1 using standard infection methods (A–C) or fusion was induced at the plasma membrane (D–F). Expression of the IAV NP protein was assessed at 8hpi by flow cytometric analysis. (A, B, D and E). N = 3 independent experiments performed in triplicate, error bars = SEM, ***p < 0.001, ns = not significant, by unpaired two-tailed *t*-test. (C and F) IAV-infected A549 cells were fixed at 8hpi and stained with anti-NP antibodies conjugated to FITC and co-stained with Hoechst 33342 before examination by confocal microscopy at 63x magnification.

endocytosis (Fig. 5A–C). When IAV infection of A549 cells was induced by fusion at the plasma membrane we observed that infection did occur, but at a decreased rate (16.0 % of cells positive for IAV NP) when compared to entry via the normal endocytic route (65.7 % of cells positive for IAV NP) (Fig. 5B and E). Intriguingly there was no significant difference in the percentage of IAV-infected cells between the PRSE- and mock-treated groups when IAV infection occurred via fusion at the plasma membrane (Fig. 5D–F). Our conclusion from these experiments, and those described in Fig. 4, is that the antiviral effect we observe upon PRSE treatment during IAV infection is due to the impact of PRSE on clathrin-mediated endocytosis. We show that if IAV entry occurs via

fusion at the plasma membrane then the antiviral effect of PRSE is negated.

3.6. PRSE treatment inhibits the replication of RSV and HMPV, but not PIV-3

Based on our observations above and our proposal that PRSE perturbs clathrin-mediated endocytosis, we aimed to test this hypothesis on select respiratory viruses that infect cells via different entry mechanisms. We chose RSV Long (Gutierrez-Ortega et al., 2008) and the low-pH dependent HMPV strain CAN97-83 (Schowalter et al., 2009)

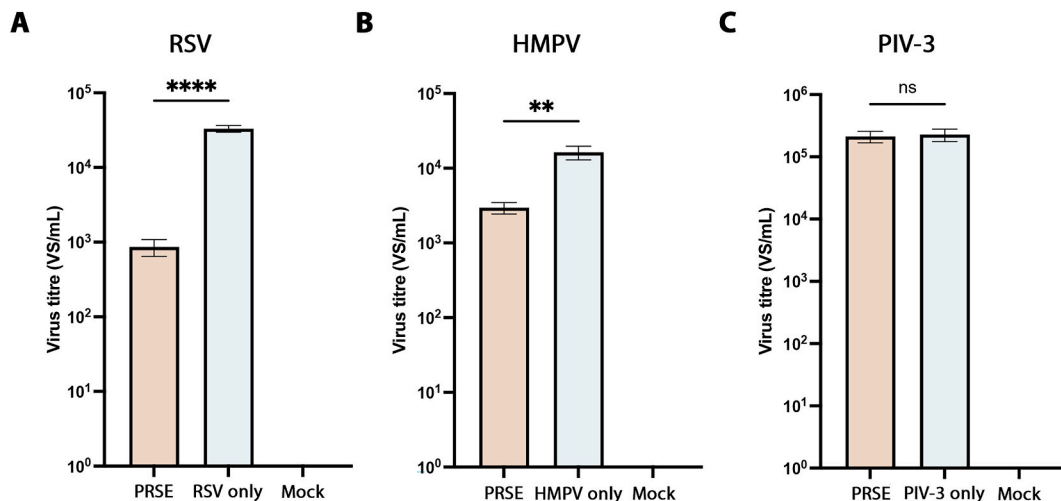


Fig. 6. PRSE treatment inhibits the replication of RSV and HMPV, but not PIV-3. A549 cells were infected with PRSE pre-treated (A) RSV Long at MOI 0.5, (B) HMPV at MOI 0.1 or (C) PIV-3 at MOI 0.01. PRSE was maintained in the culture media for the duration of infection and the amount of infectious virus was quantitated at 30hpi by virospot assay. N = 3 independent experiments performed in triplicate, error bars = SEM, **p < 0.01, ****p < 0.0001, ns = not significant, by unpaired two-tailed *t*-test.

that enter via clathrin-mediated endocytosis, and PIV-3 that enters via fusion at the plasma membrane (Meischel et al., 2021).

All three viruses were able to productively infect A549 cells as assessed using a virospot assay to quantitate the amount of infectious virus present in cell-free supernatants harvested 30hpi (Fig. 6A–C). However, upon PRSE treatment of A549 cells there was a significant reduction in the recovery of infectious RSV and HMPV (Fig. 6A and B), where PRSE treatment reduced the titre of RSV by 1.5 logs (Fig. 6A) and HMPV by ~ 1 log (Fig. 6B). Intriguingly, both RSV and HMPV are reported to utilise clathrin-mediated endocytosis for entry into host cells (Gutierrez-Ortega et al., 2008; Schowalter et al., 2009). In contrast, PRSE treatment of A549 cells did not significantly inhibit PIV-3 growth (Fig. 6C). As PIV-3 is reported to enter A549 cells by fusion at the plasma membrane (Meischel et al., 2021), these data are consistent with PRSE attenuation of clathrin-mediated entry only.

Overall, using select human respiratory viruses with different modes of cell entry we have shown that PRSE restricts the replication of IAV, RSV and HMPV but not PIV-3. This differential sensitivity appears to be related to the modes of infectious entry into host cells where IAV, RSV and HMPV are able to utilise clathrin-mediated endocytosis in contrast to PIV-3, which primarily enters via fusion at the plasma membrane.

4. Discussion

In recent years, with the high genetic variability of viruses and the emerging resistance to existing antiviral treatments, there is an increasing need to identify and develop novel antivirals. In this study, we have identified a potential MOA for PRSE, such that the antiviral activity appears to restrict and/or attenuate entry of molecules and viruses via clathrin-mediated endocytosis (Figs. 4–6). As many viruses utilise this cellular pathway for entry, we speculate that PRSE has the potential to be a broad-spectrum antiviral candidate. We demonstrated the antiviral activity of PRSE against a panel of respiratory viruses that also utilise endocytosis for entry including IAV, RSV and HMPV.

Previously, we reported that PRSE has an inhibitory effect against IAV in MDCK cells (Tang et al., 2024), but did not investigate antiviral activity in human cell lines. In this study, we confirmed the inhibitory effect of PRSE at the early stages of infection that lead to reduced IAV protein expression and subsequent virus release. We also sought to elucidate the mechanism of action of PRSE by examining the impact of PRSE treatment on the cellular antiviral response as well as the virus replication cycle.

We initially assessed STAT1 protein expression and phosphorylation upon type I IFN stimulation as an indication of induction of the cellular antiviral response. Upon stimulation of cells with PRSE alone we observed no induction of the IFN response but intriguingly, we observed a mildly enhanced expression of phosphorylated STAT1 protein in the presence of type I IFN, and this enhancement effect was even stronger in the context of IAV infection. However, our qPCR analysis on downstream ISG-signalling, which was represented by the selected ISGs MxA, OASL and IFITM3, revealed that PRSE treatment had minimal or no synergistic effect on the regulation of ISG expression after stimulation of cells with type I IFN for 6 and 24h. This is also supported by our previous study which showed PRSE-pre-treatment of cells before infection does not inhibit IAV replication (Tang et al., 2024). Overall, the anti-IAV effect of PRSE treatment is not likely to be associated with the modulation or induction of the cellular IFN antiviral responses in A549 cells.

Next, we investigated the impact of PRSE treatment on the virus replication cycle. Based on Fig. 1C–E and our previous study (Tang et al., 2024), PRSE restricts IAV replication at an early stage without affecting virus attachment. Therefore, we focused on the key viral entry pathways, caveolin-mediated and clathrin-mediated endocytosis. Our findings showed that PRSE did not affect CTB-AF647 uptake (caveolin-mediated) but impeded TF-AF647 uptake (clathrin-mediated). To confirm that disrupting clathrin-mediated endocytosis contributes to

the anti-IAV effect of PRSE, we performed an entry-bypass infection whereby virus uptake by clathrin-mediated endocytosis was inhibited, and virus entry was instead facilitated by fusion with the plasma membrane. Under these conditions we observed that IAV could still productively infect and replicate within the PRSE-treated cells (Fig. 5). These results suggest that PRSE's antiviral effect against IAV is likely due to its suppression of clathrin-mediated endocytosis.

To further evaluate the antiviral activity of PRSE and to support our observations that PRSE inhibits viral replication by perturbing clathrin-mediated endocytosis, we selected RSV and HMPV, which were reported to enter host cells via receptor-mediated endocytosis, and PIV-3, which enters host cells via fusion at the plasma membrane to test with PRSE (Cadena-Cruz et al., 2023; Cox and Williams, 2013; Meischel et al., 2021; Mo et al., 2021; Schowalter et al., 2009; Yang et al., 2016). Our results showed that PRSE treatment was selectively effective against RSV and HMPV replication, but not PIV-3 replication. These results suggest that the clathrin-mediated endocytic pathway operating during viral replication is a putative target of the antiviral activity of PRSE. Our current research aims to investigate other virus families that utilise this entry process to expand the spectrum of viruses that are susceptible to PRSE treatment.

While these findings provide compelling evidence relating to the mechanism underpinning the antiviral activity of PRSE, there are still several limitations of our study that open up promising avenues for future research. Although we have shown that IAV, HMPV and RSV are sensitive to PRSE treatment, due to the complexity of the composition of PRSE, we cannot completely conclude that the antiviral activity of PRSE is solely dependent on the blockage of virus entry. Our subsequent analyses will aim to further dissect the MOA of PRSE against identified sensitive viruses and virus families to confirm these observations. Moreover, we will aim to determine the detailed composition of PRSE with the ambition to identify the effective ingredient(s) which accounts for the antiviral activity.

5. Conclusions

In conclusion, we show that PRSE treatment does not significantly modulate the host antiviral response, but rather, appears to perturb clathrin-mediated endocytosis to inhibit virus infection. This is consistent with PRSE exhibiting an inhibitory effect against IAV, RSV and HMPV, but not PIV-3 *in vitro*. However, the possibility that PRSE acts on other stages of virus replication for different virus families cannot be fully excluded.

CRedit authorship contribution statement

Caolingzhi Tang: Writing – review & editing, Writing – original draft, Visualization, Methodology, Investigation, Formal analysis, Data curation. **Matthew Flavel:** Writing – review & editing, Supervision, Resources. **Sarah L. Londrigan:** Writing – review & editing, Writing – original draft, Validation, Supervision, Project administration, Methodology, Funding acquisition, Formal analysis, Conceptualization. **Jason M. Mackenzie:** Writing – review & editing, Writing – original draft, Supervision, Project administration, Funding acquisition, Formal analysis, Conceptualization.

Data availability

Data will be made available on request.

Funding

Funding was provided by The Product Makers to S.L.L and J.M.M. to undertake this research.

Declaration of competing interest

This research was supported by funding from The Product Makers. M.F. is employed by The Product Makers. All other co-authors have no competing interests.

Acknowledgments

The authors kindly thank and acknowledge the input of Patrick Reading (WHO CCRRI, Australia) and for the provision of influenza viruses, Kirsten Spann (Queensland University of Technology, Australia) for generous provision of the Human metapneumovirus (HMPV) strain CAN-1993/87, and Keith Chappell (University of Queensland, Australia) for the RSV specific antibody. The authors acknowledge the facilities, and the scientific and technical assistance of the University of Melbourne's Biological Optical Microscopy Platform (BOMP) and the Melbourne Cytometry Platform.

Appendix A. Supplementary data

Supplementary data to this article can be found online at <https://doi.org/10.1016/j.virol.2025.110500>.

References

- Ahtesh, F.B., Stojanovska, L., Feehan, J., de Courten, M.P., Flavel, M., Kitchen, B., Apostolopoulos, V., 2020. Polyphenol rich sugar cane extract inhibits bacterial growth. *Pril (Makedon Akad Nauk Umet Odd Med Nauki)* 41, 49–57.
- Cadena-Cruz, C., Villarreal Camacho, J.L., De Avila-Arias, M., Hurtado-Gomez, L., Rodriguez, A., San-Juan-Vergara, H., 2023. Respiratory syncytial virus entry mechanism in host cells: a general overview. *Mol. Microbiol.* 120, 341–350.
- Chan, K.F., Carolan, L.A., Druce, J., Chappell, K., Watterson, D., Young, P., Korenkov, D., Subbarao, K., Barr, I.G., Laurie, K.L., Reading, P.C., 2018. Pathogenesis, humoral immune responses, and transmission between cohoused animals in a ferret model of human respiratory syncytial virus infection. *J. Virol.* 92.
- Cox, R.G., Williams, J.V., 2013. Breaking in: human metapneumovirus fusion and entry. *Viruses* 5, 192–210.
- Deseo, M.A., Elkins, A., Rochfort, S., Kitchen, B., 2020. Antioxidant activity and polyphenol composition of sugarcane molasses extract. *Food Chem.* 314, 126180.
- Ding, Y., Cao, Z., Cao, L., Ding, G., Wang, Z., Xiao, W., 2017. Antiviral activity of chlorogenic acid against influenza A (H1N1/H3N2) virus and its inhibition of neuraminidase. *Sci. Rep.* 7, 45723.
- Elliott, S., Olufemi, O.T., Daly, J.M., 2023. Systematic review of equine influenza A virus vaccine studies and meta-analysis of vaccine efficacy. *Viruses* 15.
- Gillespie, L., Gerstenberg, K., Ana-Sosa-Batiz, F., Parsons, M.S., Farrukee, R., Krabbe, M., Spann, K., Brooks, A.G., Londrigan, S.L., Reading, P.C., 2016. DC-SIGN and L-SIGN are attachment factors that promote infection of target cells by human metapneumovirus in the presence or absence of cellular glycosaminoglycans. *J. Virol.* 90, 7848–7863.
- Griffiths, C., Drews, S.J., Marchant, D.J., 2017. Respiratory syncytial virus: infection, detection, and New options for prevention and treatment. *Clin. Microbiol. Rev.* 30, 277–319.
- Gutierrez-Ortega, A., Sanchez-Hernandez, C., Gomez-Garcia, B., 2008. Respiratory syncytial virus glycoproteins uptake occurs through clathrin-mediated endocytosis in a human epithelial cell line. *Virology* 475, 127.
- Hu, X., Li, J., Fu, M., Zhao, X., Wang, W., 2021. The JAK/STAT signaling pathway: from bench to clinic. *Signal Transduct. Targeted Ther.* 6, 402.
- Husain, M., 2024. Influenza virus host restriction factors: the ISGs and non-ISGs. *Pathogens* 13.
- Itoh, A., Sadanari, H., Takemoto, M., Matsubara, K., Daikoku, T., Murayama, T., 2018. Tricin inhibits the CCL5 induction required for efficient growth of human cytomegalovirus. *Microbiol. Immunol.* 62, 341–347.
- Ji, J., Flavel, M., Yang, X., Chen, O.C.Y., Downey, L., Stough, C., Kitchen, B., 2020. A polyphenol rich sugarcane extract as a modulator for inflammation and neurological disorders. *PharmaNutrition* 12.
- Ji, J., Yang, X., Flavel, M., Shields, Z.P., Kitchen, B., 2019. Antioxidant and anti-diabetic functions of a polyphenol-rich sugarcane extract. *J. Am. Coll. Nutr.* 38, 670–680.
- Kavanagh, K.T., Cormier, L.E., Pontus, C., Bergman, A., Webley, W., 2024. Long COVID's impact on patients, workers, & society: a review. *Medicine (Baltim.)* 103, e37502.
- Kumari, R., Sharma, S.D., Kumar, A., Ende, Z., Mishina, M., Wang, Y., Falls, Z., Samudrala, R., Pohl, J., Knight, P.R., Sambhara, S., 2023. Antiviral approaches against influenza virus. *Clin. Microbiol. Rev.* 36, e0004022.
- Lampejo, T., 2020. Influenza and antiviral resistance: an overview. *Eur. J. Clin. Microbiol. Infect. Dis.* 39, 1201–1208.
- Mazel-Sanchez, B., Niu, C., Williams, N., Bachmann, M., Choltus, H., Silva, F., Serre-Beinier, V., Karenovics, W., Iwaszkiewicz, J., Zoete, V., Kaiser, L., Hartley, O., Wehrle-Haller, B., Schmolke, M., 2023. Influenza A virus exploits transferrin receptor recycling to enter host cells. *Proc. Natl. Acad. Sci. USA* 120.
- Meischel, T., Fritzl, S., Villalon-Letelier, F., Tessema, M.B., Brooks, A.G., Reading, P.C., Londrigan, S.L., 2021. IFITM proteins that restrict the early stages of respiratory virus infection do not influence late-stage replication. *J. Virol.* 95. <https://doi.org/10.1128/jvi.00837-00821>.
- Mo, S., Tang, W., Xie, J., Chen, S., Ren, L., Zang, N., Xie, X., Deng, Y., Gao, L., Liu, E., 2021. Respiratory syncytial virus activates Rab5a to suppress IRF1-dependent IFN- λ production, subverting the antiviral defense of airway epithelial cells. *J. Virol.* 95.
- Mohamadian, M., Chiti, H., Shoghli, A., Biglari, S., Parsamanesh, N., Esmaeilzadeh, A., 2021. COVID-19: virology, biology and novel laboratory diagnosis. *J. Gene Med.* 23, e3303.
- Murayama, T., Li, Y., Takahashi, T., Yamada, R., Matsubara, K., Tuchida, Y., Li, Z., Sadanari, H., 2012. Anti-cytomegalovirus effects of tricin are dependent on CXCL11. *Microb. Infect.* 14, 1086–1092.
- Naseer, S., Khalid, S., Parveen, S., Abbass, K., Song, H., Achim, M.V., 2022. COVID-19 outbreak: impact on global economy. *Front. Public Health* 10, 1009393.
- Peteranderl, C., Herold, S., Schmolde, C., 2016. Human influenza virus infections. *Semin. Respir. Crit. Care Med.* 37, 487–500.
- Prakash, M.D., Stojanovska, L., Feehan, J., Nurgali, K., Donald, E.L., Plebanski, M., Flavel, M., Kitchen, B., Apostolopoulos, V., 2021. Anti-cancer effects of polyphenol-rich sugarcane extract. *PLoS One* 16, e0247492.
- Schalkwijk, H.H., Snoeck, R., Andrei, G., 2022. Acyclovir resistance in herpes simplex viruses: prevalence and therapeutic alternatives. *Biochem. Pharmacol.* 206, 115322.
- Schmoele-Thoma, B., Zareba, A.M., Jiang, Q., Maddur, M.S., Danaf, R., Mann, A., Eze, K., Fok-Seang, J., Kabir, G., Catchpole, A., Scott, D.A., Gurtman, A.C., Jansen, K.U., Gruber, W.C., Dormitzer, P.R., Swanson, K.A., 2022. Vaccine efficacy in adults in a respiratory syncytial virus challenge study. *N. Engl. J. Med.* 386, 2377–2386.
- Schowalter, R.M., Chang, A., Robach, J.G., Buchholz, U.J., Dutch, R.E., 2009. Low-pH triggering of human metapneumovirus fusion: essential residues and importance in entry. *J. Virol.* 83, 1511–1522.
- Schuster, J.E., Williams, J.V., 2014. Human metapneumovirus. *Microbiol. Spectr.* 2.
- Tang, C., Carrera Montoya, J., Fritzl, S., Flavel, M., Londrigan, S.L., Mackenzie, J.M., 2024. Polyphenol rich sugarcane extract (PRSE) has potential antiviral activity against influenza A virus in vitro. *Virology* 590, 109969.
- Tomba, D.R., Immanuel, A., Srikanth, S., Kadhirvel, S., 2021. Trends and strategies to combat viral infections: a review on FDA approved antiviral drugs. *Int. J. Biol. Macromol.* 172, 524–541.
- Wang, S., Ling, Y., Yao, Y., Zheng, G., Chen, W., 2020. Luteolin inhibits respiratory syncytial virus replication by regulating the MIR-155/SOCS1/STAT1 signaling pathway. *Virology* 531, 177–187.
- Wernick, N.L.B., Chinnapan, D.J.F., Cho, J.A., Lencer, W.I., 2010. Cholera toxin: an intracellular journey into the cytosol by way of the endoplasmic reticulum. *Toxins* 2, 310–325.
- Xiao, H., Killip, M.J., Staeheli, P., Randall, R.E., Jackson, D., 2013. The human interferon-induced MxA protein inhibits early stages of influenza A virus infection by retaining the incoming viral genome in the cytoplasm. *J. Virol.* 87, 13053–13058.
- Yang, H., He, H., Tan, B., Liu, E., Zhao, X., Zhao, Y., 2016. Human metapneumovirus uses endocytosis pathway for host cell entry. *Mol. Cell. Probes* 30, 231–237.
- Ye, J., Chen, J., 2021. Interferon and hepatitis B: current and future perspectives. *Front. Immunol.* 12, 733364.